Available online at www.sciencedirect.com
SCIENCE DIRECT
Experimental Eye Research 80 (2005) 259–272
EXPERIMENTAL EYE RESEARCH
www.elsevier.com/locate/yexer

Quantifying rod photoreceptor-mediated vision in retinal degenerations: dark-adapted thresholds as outcome measures

Alejandro J. Roman[1], Sharon B. Schwartz[1], Tomas S. Aleman, Artur V. Cideciyan, John D. Chico, Elizabeth A.M. Windsor, Leigh M. Gardner, Gui-shuang Ying, Elaine E. Smilko, Maureen G. Maguire, Samuel G. Jacobson*

Department of Ophthalmology, Scheie Eye Institute, University of Pennsylvania, Philadelphia, PA 19104, USA

Received 20 July 2004; received in revised form 15 September 2004; accepted 21 September 2004
Available online 18 November 2004

Abstract

Pre-clinical trials of treatment in retinal degenerations have shown progress toward preventing loss or restoring function of rod photoreceptors. In anticipation of human clinical trials, we assessed two psychophysical methods of quantifying rod photoreceptor-mediated function as potential outcome measures. Modified automated perimeters were used to deliver focal or full-field light stimuli and dark-adapted thresholds were measured. Patients with retinal degeneration were studied in two experimental protocols. Experiment 1 ($n=35$ patients) studied dark-adapted focal chromatic stimuli in central retinal locations along the horizontal meridian. Experiment 2 ($n=146$ patients) studied dark-adapted responses to a full-field stimulus test (FST) using white and chromatic stimuli. Patients in both experimental groups had testing on two different visits to determine inter-visit variability. In Experiment 1, two subgroups of patients were identified: a group with a majority of test loci detected by rod photoreceptors and a group with only cone-mediated detection. Inter-visit variability (95% confidence interval) was $\pm 3{\cdot}1$ dB for normals, $\pm 3{\cdot}0$ dB for patients with rod-mediated function and $\pm 2{\cdot}8$ dB for patients with only cone-mediated function. In Experiment 2, the dynamic range of the FST using white stimuli was sufficient to quantify sensitivity in all patients studied, including those with severe retinal degenerations. Chromatic stimuli in the FST were detectable by 85% of patients and rod- or cone-mediation could be determined. Regional retinal sources of FST were explored by comparing FST and dark-adapted perimetry in the same patients; there was a strong correlation between FST level and the loci with highest sensitivity by perimetry. Inter-visit variability (95% confidence interval) in the patients was $\pm 3{\cdot}9$ dB compared to $\pm 3{\cdot}5$ dB in normals. Dark-adapted focal threshold measurements with an abbreviated protocol in retinal degeneration patients with stable fixation may be useful as an outcome measure for therapies that can affect rod vision. FST measurements were feasible and reproducible in a large spectrum of retinal degenerative diseases and will be most applicable as a psychophysical outcome measure for treatment trials of very severe disorders in which fixation is lost and there is need for a large dynamic range of stimulus intensity.

Keywords: cone; Leber congenital amaurosis; perimetry; retinitis pigmentosa; rod

1. Introduction

Progress toward therapy for retinal degenerative diseases has accelerated in recent years and clinical trials of novel therapeutic strategies are ongoing or planned (Bessant et al., 2001; Margalit et al., 2002; Humayun et al., 2003; Weleber et al., 2003; Delyfer et al., 2004). Some future therapies will target the rod photoreceptor or are expected to affect rod function, thus making rod photoreceptor-mediated vision worth measuring to determine efficacy as well as safety. To date, the primary outcome measures in larger trials of nutrient therapies in retinitis pigmentosa (RP) have been cone function measurements (Berson et al., 1993, 2004; Hoffman et al., 2004).

Rod-specific measures of visual function that are potentially useful for assessing therapeutic effects in retinal degenerative diseases, such as RP, include the rod

* Corresponding author. Dr Samuel G. Jacobson, Scheie Eye Institute, 51 North 39th Street, Philadelphia, PA 19104, USA.
E-mail address: jacobsos@mail.med.upenn.edu (S.G. Jacobson).
[1] These authors contributed equally to the work.

0014-4835/$ - see front matter © 2004 Elsevier Ltd. All rights reserved.
DOI:10.1016/j.exer.2004.09.008

electroretinogram (ERG) and rod-mediated psychophysics. The rod ERG b-wave, a surrogate measure of rod vision across the entire retina, is recordable in many RP patients and has been shown to be a robust measure (Berson et al., 1985, 1993; Birch et al., 1991, 1999, 2002; Grover et al., 2003; Hoffman et al., 2004). Once peripheral retinal function becomes impaired in RP, there may be no measurable rod ERG and this can occur at relatively early disease stages. Although bright light stimuli could elicit residual rod ERG function, the recorded signal is complex and tends to have both rod and cone components. Unlike the cone flicker ERG, the rod ERG is not amenable to the strategy of delivering scores of stimuli at short inter-stimulus intervals to record small signals by averaging methods because of complexities introduced by light adaptation.

Dark-adapted psychophysics has a long history of study by visual scientists seeking knowledge of the limits of visual perception (Cornsweet, 1970) and has a traditional role in clinical settings to determine dark-adapted thresholds, usually to a relatively large achromatic stimulus within the central field (Marmor et al., 1983). Dark-adapted chromatic perimetry has been used in many investigations of retinal degeneration to distinguish rod- from cone-mediated function across the visual field of patients of unknown genotypes and subsequently in those with known molecular causes (e.g. Gunkel, 1967; Massof and Finkelstein, 1979; Lyness et al., 1985; Jacobson et al., 1986, 1991, 2000; Birch et al., 1987; Cideciyan et al., 1998). It would seem logical to try to transfer a version of the technique from this research role to that of a clinical outcome measure. Progress toward this goal has already been made (Birch et al., 1999).

The current work addresses the need for psychophysical methodology to assess rod photoreceptor-mediated vision for future clinical trials in patients with retinal degeneration. Two different dark-adapted psychophysical strategies are assessed for feasibility as candidate outcome measures: one using focal stimuli which provide spatial information about function in the central retina, and a second that employs a full-field stimulus and thereby no spatial information.

2. Materials and methods

2.1. Subjects

Patients with inherited retinal degenerations (Table 1) and visually normal subjects participated in the experiments. In Experiment 1, 35 patients (16 female, 19 male) and 20 normal subjects (11 female, 9 male; ages 19–55) underwent dark-adapted testing with focal chromatic stimuli in the central retina in one eye on two visits separated by no more than 6 months. In Experiment 2, 146 patients (75 female, 71 male) and 12 normal subjects (6 female, 6 male; ages 10–56) underwent a full-field stimulus test (FST) in one eye. A subset of 41 of these patients and 10 normal subjects returned within 6 months for repeat testing. Testing and retesting were performed at similar times of the day in both experimental groups. All subjects had complete ophthalmic examinations. Also performed in all patients prior to entry into the studies were kinetic perimetry (V-4e and I-4e test targets) and ERGs using a standard protocol (Jacobson et al., 1989); in all but the patients with the most severe retinal degenerations, dark-adapted two-color perimetry on a 12° grid throughout the visual field was also performed (Jacobson et al., 1986). All studies were approved by the Institutional Review Board and informed consent was obtained from all subjects after explanation of the nature of the studies. The research procedures were in accordance with institutional guidelines and the Declaration of Helsinki.

Table 1
Subject characteristics

Clinical diagnosis	Subjects (*n*)	Gender (F/M)	Age range (mean)	Subjects with two visits[a] (*n*)
Experiment 1				
Retinal degeneration[b]	35	16/19	11–61 (34)	35
Experiment 2				
Retinal degeneration[c]	112	59/53	9–81 (39)	26
Cone-rod dystrophy	16	5/11	9–66 (30)	6
Maculopathy[d]	18	11/7	18–63 (43)	9

[a] Fifteen subjects are included in both Experiments 1 and 2.
[b] Includes retinitis pigmentosa ($n=24$), Usher syndrome types I, II ($n=3$), cone–rod dystrophy ($n=2$), choroideremia ($n=6$).
[c] Includes retinitis pigmentosa ($n=78$), Leber congenital amaurosis or early onset retinal degeneration ($n=15$), Usher syndrome types I, II ($n=8$), Bardet-Biedl syndrome ($n=3$), choroideremia ($n=8$).
[d] Includes Stargardt disease ($n=13$), autosomal dominant macular degeneration ($n=3$), early onset macular drusen ($n=2$).

2.2. Testing procedures

Experiment 1 Thresholds were obtained in the dark-adapted ($\geq$45 min) state using 500 and 650 nm (1·7° diameter; 200 ms duration) stimuli on a Humphrey Field Analyzer (model 600 series; Zeiss-Humphrey Instruments, Dublin, CA) modified for this purpose (Jacobson et al., 1986). The pupils of the subjects were fully dilated (tropicamide 1%; phenylephrine 2·5%). Light-adapted testing with the same instrument but using a white stimulus early in the visit served as an explanation of the test and provided practice at performance. The full threshold strategy, a staircase algorithm available on the perimeter, was used for two-color dark-adapted static perimetry. With this bracketing strategy, stimulus intensity is initially varied in steps of 4 dB and then in steps of 2 dB. The final threshold estimate is the intensity of the last presentation seen by the patient. Details and methods of analysis have been described (Jacobson et al., 1986). Horizontal profiles, representing 25 loci, were measured across the central 60° at

2° intervals (excluding five loci at and around the blindspot). Testing time for each profile in normal subjects and patients with mainly rod-mediated function averaged 8·6 min (range, 7–12 min). The number of stimulus presentations per profile averaged 220 (range, 170–300). Testing time for those with only cone-mediated function averaged 4·5 min (range, 3–5·5 min) and number of stimulus presentations averaged 118 (range, 75–150). Fixation could not be monitored in the dark-adapted state with the Heijl-Krakau blindspot method because targets projected in the blindspot can elicit false responses to stray light. Fixation was monitored throughout examinations by infrared viewing of the patient's test eye and frequent reminders were given to maintain eye position; pauses in the testing (approximately every 2 min) occurred to avoid fatigue. False positive responding in patients and normals was similar to each other and similar on the two visits: 80–90% of subjects had no false positives. False negative responding in patients and normals followed the same pattern on both visits: 80–90% had no false negatives.

Experiment 2. Thresholds to a full-field stimulus were obtained in the dark-adapted state using white, red or blue flashes (200 ms duration) and the same full threshold strategy as in Experiment 1. The stimuli were delivered with an automated perimeter (Humphrey Field Analyzer; model 750i; Zeiss-Humphrey Instruments, Dublin, CA) modified for this purpose (see Appendix A for details of instrument modifications). Chromatic testing was performed to determine whether there was rod- or cone-mediation of detection. The color filters in the perimeter were used unmodified and the spectral characteristic of these broadband filters was measured (Appendix A, Fig. A1(F)).

Pre-testing with the white stimulus was used for explanation of the test and practice at performance. Measurements were made for each test eye in the following sequence: white, white, blue, red, white, blue, red, white. Testing time per eye for this sequence did not exceed 8 min. A subset of normal subjects ($n=2$) underwent dark (bleaching) adaptation functions following exposure to light (full-field white flash expected to isomerize 97% of rhodopsin; Cideciyan et al., 2004) to determine what the sensitivity difference would be between blue and red stimuli on the cone plateau (~4–13 min after the flash) and on rod portions of the function; this enabled interpretation of results of chromatic testing in the patients.

The relationship of FST level (using white stimuli) to results of dark-adapted two-color perimetry (72 loci) on a 12° grid (Jacobson et al., 1986; Apathy et al., 1987) from the same patients was determined. Sensitivity loss was used to compare the two sets of data. FST loss was defined as the difference between mean normal and patient FST sensitivity. Rod sensitivity losses at individual loci in the visual field were at those loci with rod- or mixed- (500 nm detected by rods; 650 nm detected by cones) mediation and results (from the 500 nm responses) were plotted as a function of eccentricity in the field for each patient. Mean field rod (500 nm) sensitivity losses were also calculated and plotted for comparison with FST losses. For the entire patient population, FST sensitivities were plotted versus the highest sensitivity (to 500 nm) among the 72 loci tested in dark-adapted perimetry.

2.3. Data analyses

Experiment 1. Difference between dark-adapted sensitivity to 500 and 650 nm stimuli at each locus was used to determine whether both stimuli were being detected by rods or by L/M (long/middle wavelength) cones, or there was mixed rod- and cone-mediation (Jacobson et al., 1986). Briefly, loci with sensitivity differences (500 nm minus 650 nm) greater than or equal to 28 dB were classified as mediated by rods, whereas differences equal to or lower than 12 dB indicated cone-mediation. Values between these limits were considered to have mixed rod- and cone-mediation. In the calculation, 16 dB was added to the measured sensitivity levels of the 500 nm stimulus to equate the energy of this stimulus to that of the 650 nm stimulus. Complete details of the calculations leading to determining photoreceptor mediation have been published (Jacobson et al., 1986; Apathy et al., 1987). Patients were divided into two subgroups for further analyses: those with cone-mediated fields and those with most loci having rod-mediation to the 500 nm stimulus; the latter subgroup usually also showed a minority of cone-mediated loci around fixation. Inter-visit variability was examined using the mean sensitivity of the dark-adapted profiles. For the rod-mediated group ($n=24$), mean sensitivity was derived from sensitivities at extrafoveal loci using the 500 nm stimulus. Loci were categorized as having no measurable sensitivity if rod sensitivity loss was greater than 30 dB based on mean locus-specific normal data. For the cone-mediated group ($n=11$), the mean sensitivity was derived from sensitivities at extrafoveal and foveal loci using the 650 nm stimulus because of the greater dynamic range of results with this stimulus color (Jacobson et al., 1986). Previous work emphasizing the artifactual truncation of variability estimates from floor effects (i.e. unmeasurable vision due to limited dynamic range of perimeter or large defect depth; Chauhan and Johnson, 1999; Spry et al., 2001; Blumenthal et al., 2003) prompted us to analyse the dark-adapted profile results using not only the full number of loci (60° field) but also an abbreviated set of central loci (16° field) with mostly measurable vision. Inter-visit variability was quantified and graphically displayed as twice the pooled standard deviation of the difference distribution (visit 2 minus visit 1) with the Bland-Altman analysis (Bland and Altman, 1986). Measurement variability of patient and control groups was also compared with an F-test of equal variance. Differences in the mean between the two visits were examined with a paired t-test (PC SAS; version 8.01, SAS Institute, Cary, NC).

Experiment 2. Within-visit variability of FST data was determined using, on average, four FST measurements at each session with the white stimulus. Variability was quantified as the within-subject standard deviation or measurement error (Bland and Altman, 1996) and calculated by one-way analysis of variance. To examine the effect of sensitivity level on within-visit variability, we plotted the individual subjects' standard deviations against their means and evaluated the association by Spearman rank correlation coefficient. Inter-visit variability of the mean of FST sensitivities to the white stimulus was determined with the Bland–Altman analysis (Bland and Altman, 1986) as in Experiment 1. To examine the effect of sensitivity level on inter-visit variability, we divided sensitivities into groups (low and high sensitivity) based on the average sensitivity of the two visits (using the median as the cutpoint) and compared the groups with an *F*-test for equality of variances. Measurement variability of patient and control groups was also compared using an *F*-test of equal variance; differences in the mean between the two visits were examined with a paired *t*-test.

3. Results

Table 1 lists clinical diagnoses of the patients included in the two experimental protocols. For Experiment 1, all patients had central fixation. For Experiment 2, the test strategy did not necessitate stable central fixation, so patients with maculopathy and severe retinal degenerations that involved both central and peripheral retina were also studied. The large number of patients with different retinal degenerations and at different disease stages included in Experiment 2 provided answers to questions about regional retinal sources and variability of this newly designed dark-adapted full-field psychophysical test.

3.1. Experiment 1: dark-adapted focal stimulus test results

Fig. 1A shows representative dark-adapted two-color profiles of sensitivity across the horizontal meridian in a normal subject and two patients with retinal degeneration. In a 22-year-old female normal subject (Fig. 1A, left),

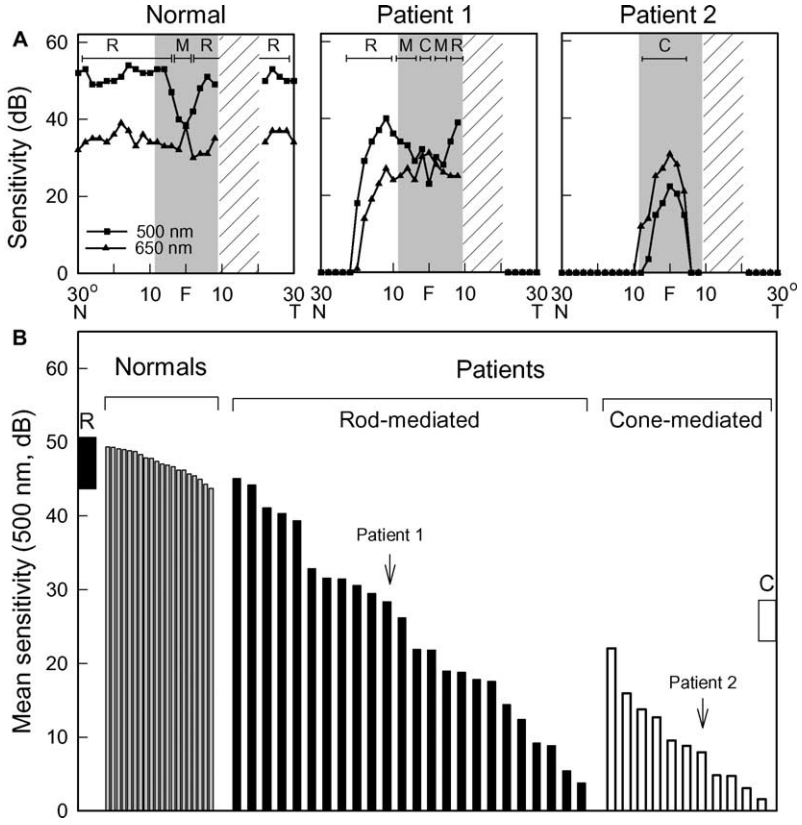

Fig. 1. Dark-adapted focal testing at loci along the horizontal meridian in retinal degenerations. (A) Representative sensitivity profiles in a normal subject and two patients with retinal degeneration (Patients 1 and 2) using 500 nm (squares) and 650 nm (triangles) stimuli. The photoreceptor mediation at each locus, based on the sensitivity difference between the two colors, is given: R, rod-mediated; M, mixed rod- and cone-mediated; C, cone-mediated. Gray zone represents the central 16° of visual field used for calculating mean sensitivities. Hatched area is region around and including the physiological blindspot. F, fovea; N, nasal; T, temporal. (B) Mean sensitivities (central gray zone; 500 nm stimulus) in the 35 patients compared with a group of 20 normal subjects. Patients are subdivided by whether their function is mainly mediated by rod photoreceptor pathways (rod-mediated; filled bars) or L/M cone pathways (cone-mediated; unfilled bars). Bars on vertical axes show mean normal sensitivity (± 2SD) for rod-mediation (R, left) and cone-mediation (C, right). Patients 1 and 2, whose data are shown in (A), are identified.

extrafoveal sensitivities for both 500 and 650 nm stimuli are mediated by rod (R) photoreceptors. A 30-year-old female patient with Usher syndrome (Fig. 1A, Patient 1) has reduced sensitivities to the 500 nm stimulus and detection is mediated by rod photoreceptors except at the foveal locus, which is cone-mediated. Beyond 12° and 18° in the nasal field, there is a transition from high sensitivity to no measurable vision; after 8° in the temporal field, there is the designated blindspot region and thus no data. A 38-year-old male patient with RP, in contrast, has no measurable rod-mediated function and the loci with detectable sensitivity are cone-mediated (Fig. 1A, Patient 2). Peak sensitivity is at the foveal locus and there is a decline in sensitivity to no measurable vision within 10° nasal and temporal from the fovea. We quantified the horizontal extent of functioning retina in the two patient subgroups to limit further data analyses to zones of measurable vision. Among the patients with rod-mediated detection, ≥80% of eyes had measurable function at eccentricities up to 4°; the percentage declined to ≥45% by 8° and was lower at further eccentricities. Among the patients with only cone-mediated function, there was also a decline in percentage of eyes with measurable function from ≥90% at 4° to ≥45% at 6° eccentricity; by 8°, only about 20% of eyes had responses. The central 16° of field tested thus had the most measurable function in both patient subgroups and was used for further analyses (gray zone in Figs. 1 and 2A). The spectrum of dysfunction within the central 16° is shown for patients (Fig. 1B). Within the rod-mediated group, there are patients whose data fall within normal limits (mean normal, 47·1 dB; SD, 1·72 dB), but 22 of 24 patients are abnormally reduced in sensitivity. There is also a range of dysfunction within the subgroup of patients with only cone-mediated function; all patients have mean data that are subnormal.

Dark-adapted profiles from two different visits for a 34-year-old normal male subject and the previously depicted patients with retinal degeneration show that, by inspection, the results of testing and repeat testing appear similar (Fig. 2A). Inter-visit variability analyses in normal subjects and the two subgroups of patients are shown (Fig. 2B). We used the mean sensitivity of the central test region with highest percentages of measurable loci (central 16° of field; gray zone in Figs. 1 and 2A), so as not to introduce floor effects from the unmeasurable zones that would cause artifactually reduced estimates of variability (Chauhan and Johnson, 1999; Spry et al., 2001; Blumenthal et al., 2003). For the 20 normal subjects (Fig. 2B, left), the mean sensitivity difference (±SD) is −0·01 (±1·55) dB. The difference in mean sensitivity is not significantly different from zero ($p=0·97$). For the subgroup of 24 patients with mainly rod-mediated function (Fig. 2B, middle), the mean sensitivity difference (±SD) is 0·52 (±1·52) dB, which is not different from zero ($p=0·11$). For the subgroup of 11 patients with only cone-mediated function (Fig. 2B, right), inter-visit variability analyses (using 650 nm stimulus data) have a mean

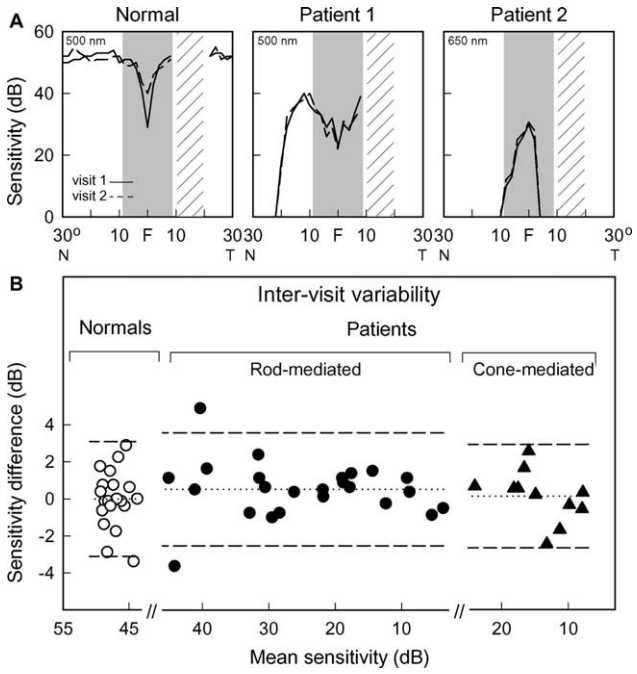

Fig. 2. Inter-visit variability of dark-adapted focal testing in retinal degenerations. (A) Representative sensitivity profiles across the horizontal meridian on two different visits in a normal subject and the two patients with retinal degeneration (from Fig.1). Gray zone delimits central 16° of visual field used for inter-visit variability analyses. Visit 1, continuous lines; visit 2, dashed lines. F, fovea; N, nasal; T, temporal. (B) Sensitivity difference between visits (visit 2 minus visit 1) as a function of mean sensitivity of the two visits in 20 normal subjects (unfilled circles; 500 nm data), 24 patients with rod-mediated function (filled circles; 500 nm data) and 11 patients with cone-mediated function (filled triangles; 650 nm data). Dotted line is mean sensitivity difference; dashed lines represent ±2SD.

sensitivity difference (±SD) of 0·14 (±1·40) dB and this is not significantly different from zero ($p=0·74$). A comparison of measurement variability between the three groups shows that rod-mediated and cone-mediated groups do not differ ($p=0·80$); there is also no difference between inter-visit variability in the normal group and either the rod-mediated group ($p=0·93$) or cone-mediated group ($p=0·76$). If all 24 extrafoveal loci from the dark-adapted profiles are used in the calculation of inter-visit variability, the following mean sensitivity differences (±SD) are obtained: normal subjects, −0·34 (±1·01) dB; rod-mediated patients, 0·20 (±0·75) dB; cone-mediated patients, 0·06 (±0·51) dB.

3.2. Experiment 2: dark-adapted full-field stimulus test (FST) results

There was sufficient dynamic range of the FST using white stimuli to quantify visual function in all patients studied. As expected from such a wide spectrum of diseases and severities, there were different levels of visual function ranging from normal to nearly six log units subnormal (Fig. 3, upper panel). In the group of 20 patients with

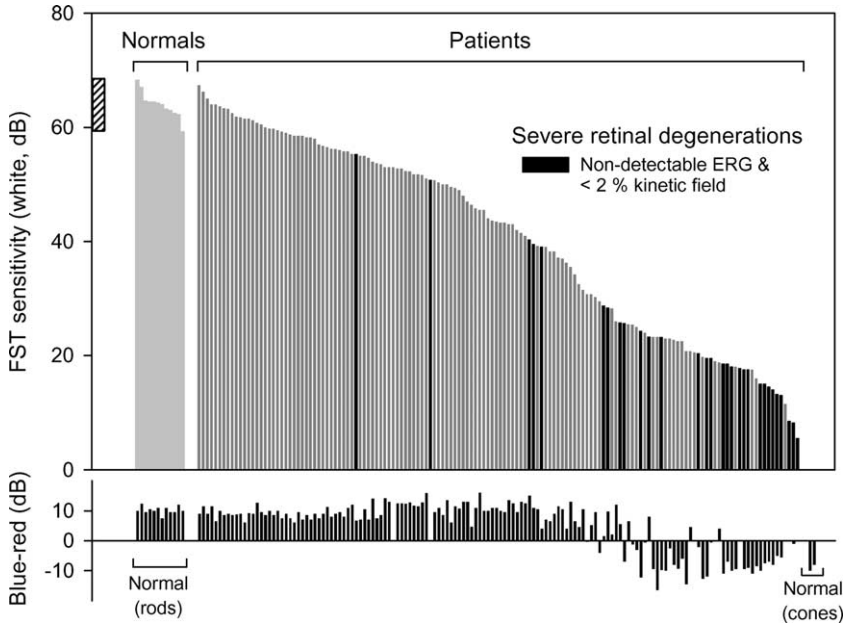

Fig. 3. Dark-adapted full-field stimulus test (FST) results in retinal degenerations. Upper. Spectrum of FST sensitivities in normal subjects ($n=12$) and patients with retinal degenerations ($n=146$), ranked from high (left) to low (right) sensitivity. Patients with the most severe retinal degenerations ($n=30$), defined by no detectable clinical ERG and very reduced extent of visual fields to both I-4e and V-4e test targets, are marked (black lines). Hatched bar on vertical axis represents mean normal FST ± 2SD Lower. Chromatic FST results are shown below each individual's white FST result as the difference between blue and red sensitivities. Like the normal results, most patients with higher white FST results have rod-mediation by the chromatic comparisons; the more severely affected patients may have rod- or cone-mediation. Normal dark-adapted cone results were obtained by performing the test on the cone plateau of dark adaptation following light exposure.

sensitivities that were within normal limits (mean normal, 63·9 dB; SD, 2·29 dB), there were 12 patients with the clinical diagnosis of inherited maculopathy, five patients with cone-rod dystrophy (CRD), and three with forms of RP. Among the 126 patients with subnormal FST results, the most frequent clinical diagnosis was RP (75 patients; 60%). FST testing was feasible in all patients studied.

Chromatic FST results were also obtained to determine the feasibility of estimating photoreceptor mediation of the full-field responses (Fig. 3, lower panel). The difference in sensitivities to blue and red stimuli (e.g. Massof and Finkelstein, 1979; Ernst et al., 1983; Jacobson et al., 1986; Birch et al., 1987) is used to determine rod versus L/M cone mediation. Normal dark-adapted subjects, who would be expected to use rod-mediated vision to detect these stimuli, show higher sensitivity to blue than to red; the difference in sensitivities averages 10·2 (SD, 1·3 dB). The sensitivity difference for L/M cone mediation of FST chromatic stimuli was determined in two normal subjects tested on the cone plateau of a dark adaptation function; both showed red sensitivity greater (by 10 and 8 dB) than that of blue. In the 125 patients who were able to detect both blue and red stimuli, 105 patients showed differences that were positive and this is taken as evidence that rods were the predominant photoreceptor type mediating FST detection (assuming that responses to the two stimuli were from the same retinal region). Patients with the lowest FST results to white tended to show a different response pattern to the chromatic stimuli than those with higher sensitivities. These patients had higher sensitivity to red than blue, making it likely that their residual vision was L/M cone-mediated (also confirmed in many such patients by dark-adapted two-color perimetry; data not shown).

What are the FST responses in patients with more severe retinal degenerative disease, defined as having both a non-detectable ERG and very limited visual field extent by kinetic perimetry? Among the 30 patients with severe retinal degenerations so defined, all had detectable FST responses using white stimuli (Fig. 3). In the 17 patients who were able to detect both blue and red stimuli, 9 patients (53%) were rod-mediated and 8 (47%) were cone-mediated; a further 10 patients only detected the red stimulus and were likely to have cone-mediation. The subgroup of patients with the diagnosis of Leber congenital amaurosis or early onset retinal degeneration ($n=15$; ages 11–47) is worthy of specific mention. Some patients in this clinical diagnostic category had markedly reduced but detectable ERGs and therefore were not considered severe by the above definition. By kinetic perimetry (V-4e test target), the 15 patients could retain detectable small central islands or peripheral islands or both. FST results to the achromatic stimulus were all abnormally reduced. Chromatic FST showed that nine patients detected both blue and red stimuli and eight of these were rod-mediated and one cone-mediated; six only

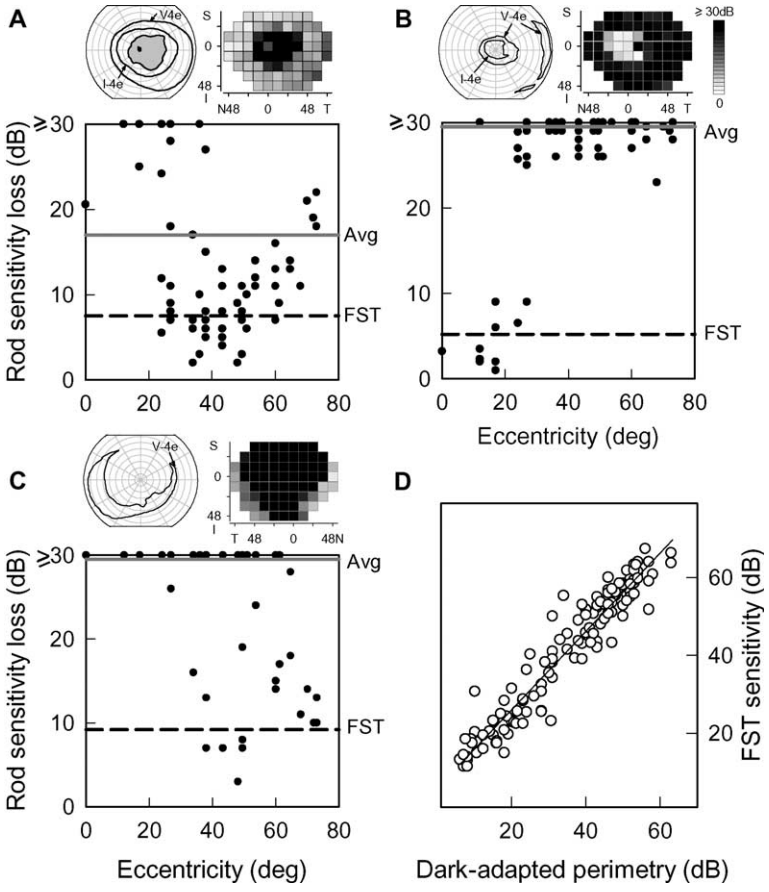

Fig. 4. Regional retinal sources of FST results. Spatial data from the visual fields of three representative patients with retinal degeneration (A–C) are shown and compared with FST results. For each patient, there is a kinetic field using two target sizes (upper left in each data group), gray scale map of rod sensitivity losses from dark-adapted perimetry (upper right), and graph of rod sensitivity losses versus eccentricity (lower). Relative scotomas are shown as gray in kinetic fields. Gray scale for maps of rod sensitivity loss is shown to the right of (B). Avg = average loss based on 72 rod sensitivity loss measurements from the dark-adapted perimetry. FST = FST loss based on comparison of mean normal and patient FST sensitivity. (D) Testing the hypothesis that FST results are derived from the highest sensitivities in the retina. FST sensitivity for each patient is plotted against the highest sensitivity to 500 nm among the 72 loci measured in dark-adapted perimetry. Linear correlation shown.

detected the red stimulus and were likely to have cone-mediation.

The regional retinal sources of FST were explored to test the hypothesis that FST responses originate from the most sensitive retinal areas, independent of where in the retina these areas are located (Fig. 4). Data from three patients illustrate the relationship between FST results for white stimuli (all rod-mediated by blue-red sensitivity differences of 8–10 dB) and the sensitivity of individual rod-mediated loci determined by dark-adapted two-color perimetry. To compare perimetric and FST data, we graph rod sensitivity losses (RSL) against eccentricity and also displayed the FST result as loss. The average RSL across the visual field is also shown, mainly to illustrate the lack of relationship of this parameter with FST (Fig. 4A–C). A 16-year-old man with autosomal recessive CRD and visual acuity (VA) of 20/60 had a large relative central scotoma and some limitation of peripheral function by kinetic perimetry (Fig. 4A). A map of RSL and the graph of RSL versus eccentricity show that beyond the prominent central dysfunction, there was less severe loss in the mid-peripheral field but increasing dysfunction again in the far periphery. FST loss falls among the loci with least RSL on the eccentricity plot but differs by about one log unit from the average RSL. A 33-year-old man with simplex RP and VA of 20/20 had kinetic perimetry that showed a central island separated from far temporal peripheral islands by a complete annular mid-peripheral scotoma (Fig. 4B). The map of RSL and the graph indicate little if any central dysfunction but severe losses in the mid- and far-peripheral field. FST loss is accounted for by the cluster of loci with minimal or no RSL within the central 20 degrees; average RSL differs by at least 2 log units. A 45-year-old man with X-linked RP and VA of 6/200 retained an incomplete peripheral island of vision by kinetic perimetry (Fig. 4C). A map of RSL and comparison of FST loss with RSL from different eccentricities indicates that the loci in the peripheral field with minimal RSL relate most closely to the level of FST

disturbance. In the patients with data from both FST and dark-adapted perimetry, a comparison was made between FST sensitivity level (white stimulus) and the locus with maximum sensitivity from dark-adapted perimetry (500 nm stimulus). Strong linear (slope = 1·00) correlation (r = 0·96) was found in this comparison (Fig. 4D) as well as between FST sensitivities and each of four clusters of loci (averaged loci within 2, 4, 6 or 8 dB from highest sensitivity; all show $r > 0·95$), thus providing support for the hypothesis that FST is measuring the response of the most sensitive retinal areas.

Within- and inter-visit variability of FST measurements were analysed (Fig. 5). All measurements within a session for the 12 normal subjects and 146 patients are shown; data were ranked by the mean FST for that session (Fig. 5A, upper panel). The differences of each measurement from the session mean are displayed (Fig. 5A, lower panel) and do not vary with FST level. The individual subjects' standard deviations plotted against their means demonstrated they were unrelated ($r = 0·10$; $p = 0·25$). The within-subject standard deviation or measurement error (Bland and Altman, 1996) is 1·63 dB for normal subjects and 1·61 dB for the patient group; the variances are not significantly different ($p = 0·83$). Inter-visit variability for the subgroups of 10 normal subjects and 41 patients is also shown (Fig. 5B). Mean sensitivity difference (±SD) for normals is −0·82 (±1·76) dB and for patients is 0·05 (±1·95) dB, both not significantly different from zero ($p = 0·18$ and 0·86, respectively). Inter-visit variability in the patients is not dependent on mean sensitivity level ($p = 0·93$).

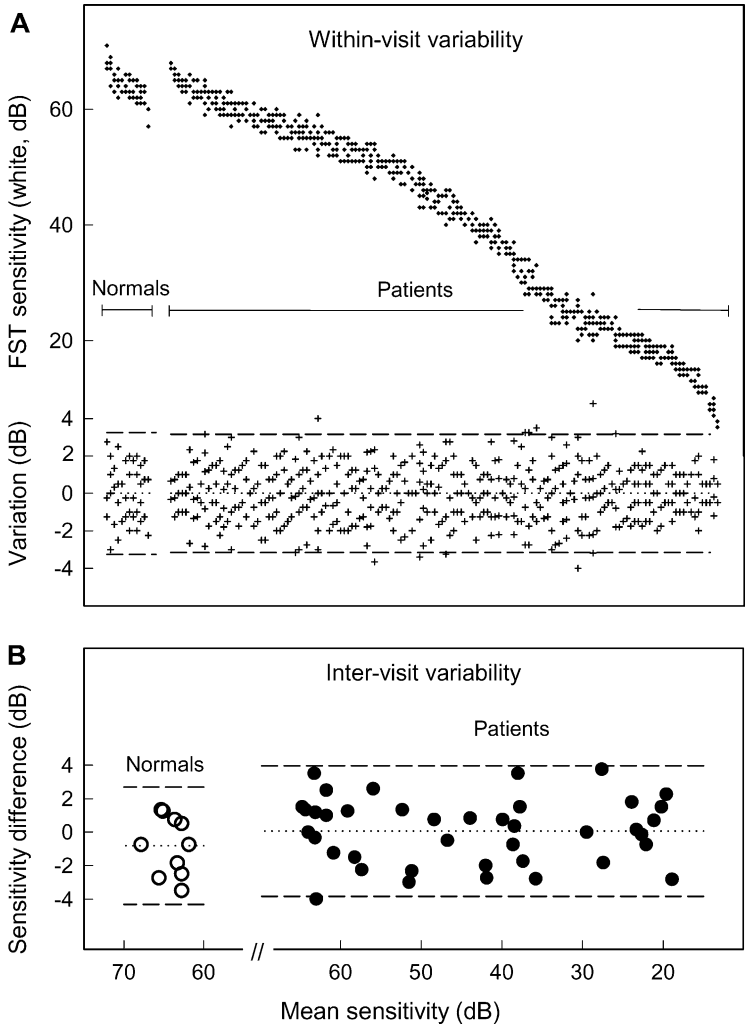

Fig. 5. Within- and inter-visit variability of FST. (A) Upper. FST white stimulus results (between 2 and 6 measures) within a single session are shown (small diamonds) for each of the 12 normal subjects and 146 patients, ranked by mean FST (from high to low). Lower. Differences of each FST measure from session mean are plotted (+) for normals and patients. Dashed lines represent mean ±2SD of the within-visit variability so calculated for the normal group and the patient group. (B) Inter-visit variability for FST white stimulus results. Sensitivity difference (visit 2 minus visit 1) is plotted as a function of mean sensitivity in 10 normal subjects (unfilled symbols) and 41 retinal degeneration patients (filled symbols). Dotted line is the mean sensitivity difference and dashed lines represent ±2SD.

4. Discussion

Dark-adapted threshold measurements to quantify rod-mediated vision are a recommended part of the ocular examination of patients with RP and related disorders (Marmor et al., 1983). Natural history studies of inherited retinal degenerations have included dark-adapted thresholds, but more data are available on cone measures, such as visual acuity, color vision, light-adapted perimetry and cone ERGs (for example, Berson et al., 1985, 2002, 2004; Holopigian et al., 1996; Birch et al., 1999; Hirakawa et al., 1999; Caruso et al., 2001; Flynn et al., 2001; Lodha et al., 2003). Only cone function, specifically the cone flicker ERG and light-adapted perimetry, has been used as the primary outcome measure in RP treatment trials to date (Berson et al., 1993, 2004; Hoffman et al., 2004). Why should there be a preference to measure cone function when rod-mediated vision would seem equally appropriate in these diseases? There are at least four contributing factors. First, cone vision testing is less time consuming and testing apparatus is more available: there is no need to wait lengthy times to dark adapt the eyes, and visual acuities and visual fields do not even require pupillary dilation. Second, light-adapted perimetry to measure cone vision across the visual field has a rich history of use in glaucoma (e.g. Spry and Johnson, 2002) and neuro-ophthalmological disease (e.g. Keltner et al., 1999), and this experience can be drawn upon. Third, a submicrovolt cone flicker ERG, after much discussion about methodology and signal origins (Andreasson et al., 1988; Dagnelie and Massof, 1994; Birch and Sandberg, 1997; Sieving et al., 1998), is generally accepted as a surrogate measure of integrated cone vision in late-stage retinal degeneration. Finally, inclusion of patients with measurable cone vision but severely diminished rod vision in studies expands the available data set for greater statistical power.

Future trials of treatment in hereditary retinal degenerations will benefit from having rod-specific as well as cone-specific outcome measures in order to understand how each photoreceptor type is affected by the intervention. As therapies emerge and become useful at earlier rather than later disease stages, there may be less need to concede the loss of rod photoreceptors and only concentrate on retaining cone function (e.g. Wong, 1997). Furthermore, successful murine preclinical experiments based on retained outer nuclear layer thickness (LaVail et al., 1998) may more appropriately translate into treatment of rod-based vision in human patients (assuming post-receptoral connectivity is intact, Marc et al., 2003) since the great majority of photoreceptor nuclei in the mouse retina are rods. The present work studied the feasibility and variability of two types of dark-adapted psychophysical threshold measurement that may be used to assess rod vision: (1) a focal stimulus method that samples a group of predefined central retinal locations and requires stable fixation; and (2) a full-field stimulus method not requiring stable fixation.

Dark-adapted two-color profile testing, as performed in Experiment 1, builds upon experience gained from earlier studies that used such profiles or greater numbers of test loci to characterize phenotypes of retinal degenerations (e.g. Massof and Finkelstein, 1979; Lyness et al., 1985; Birch et al., 1987; Apfelstedt-Sylla et al., 1992; Cideciyan et al., 1998; Jacobson et al., 2000). Considering two profiles using different wavelength stimuli were needed to determine photoreceptor-mediation, we limited the number of test loci per profile to reduce test time and avoid patient fatigue. False positive and false negative rates were similar in patients and normal subjects and like those reported for glaucoma (Katz and Sommer, 1988, 1990). Such profiles, however, may be an inappropriate choice to assess outcome in many future experimental treatments in disease subsets. Flexibility in the method, though, allows ready replacement by clusters of loci or other strategies to accommodate the specific goals of a trial. For example, transition zones between good and poorly functioning retina, as in the nasal field in Patients 1 and 2 (Figs. 1A and 2A) or along the vertical meridian in class B1 *rhodopsin* gene mutations (Cideciyan et al., 1998), may be worth monitoring after a focal intervention placed to avoid degenerate retina but not to threaten well-functioning areas. Rod-mediated dark-adapted sensitivity abnormalities (Owsley et al., 2000) and rod photoreceptor pathology (Curcio et al., 1996) have been documented in age-related macular degeneration (AMD) making strategies with a macular grouping of test loci potentially useful for determining the effects of early or preventive treatment in AMD patients when fixation is present. As occurs in glaucoma assessment (Gordon and Kass, 1999; Reus and Lemij, 2004), there can be coordinated use of objective structural measurements (e.g. in vivo cross-sectional retinal imaging) in the same locations chosen for dark-adapted functional measurements (Cideciyan et al., 2004; Jacobson et al., 2004).

Sources of variability in automated light-adapted perimetry have been well-studied in relation to glaucoma (Spry and Johnson, 2002). In hereditary retinal degenerations, most published information is concerned with the variability of full-field ERG measures (Berson et al., 1985, 1993; Birch et al., 1991, 1999, 2002; Hoffman et al., 2004). By data inspection, the dark-adapted profile tests appeared quite repeatable in all patients with retinal degenerations, but we sought to quantify the variability. Inter-visit variability in the group of patients with rod function is comparable to that in the normal group and the cone-mediated group. There is only one previous report of variability measurements for rod-mediated function using automated dark-adapted two-color static perimetry (Birch et al., 1999). Inter-visit variability of mean rod sensitivity was determined in 29 patients using 74 retinal locations; a threshold criterion for change (at the 95th percentile) was reported as 5·26 dB. This result could be compared with 3·05 dB in our 24 patients with rod-mediated function, sampled from eight

central field loci. The many differences between the two studies make comparisons difficult.

The full-field test of dark-adapted thresholds, as performed in Experiment 2, was born of the necessity to quantify vision in patients with severe retinal degenerations and unstable fixation, based on promising therapeutic directions (de Juan et al., 1999; Acland et al., 2001; Humayun et al., 2003). The concept of full-field dark-adapted perceptual testing is not novel and has previously been explored for glaucoma screening (Glovinsky et al., 1992) and in retinal degenerations to evaluate results of retinal transplantation or a visual prosthesis (de Juan et al., 1999; Humayun et al., 2000, 2003). The instrumentation and method in the current work was more like the published design using a Tubingen bowl perimeter (Glovinsky et al., 1992) than the modified ERG apparatus (Humayun et al., 2000); there is also a commercially available LED-based instrument but the limited dynamic range would not accommodate severe retinopathies (Peters et al., 2000). We tried to keep modifications to the automated perimeter at a minimum (see Appendix A) to enable other investigators to repeat and extend the work using equipment that would be readily available in most ophthalmic departments and private offices. The protocol was feasible in a large cohort of patients with retinal degenerations, including those with severe retinopathy. The intuitive hypothesis that FST results would emanate from the most sensitive retinal regions was tested using dark-adapted perimetry in many of the patients able to do both tests and found to be valid. Additional testing strategies will need to be devised to gain spatial information about the function in severely affected patients. A formal method and scoring system to determine light projection in different regions of the visual field, accomplished usually with a penlight (Humayun et al., 2000), may be of value. A suprathreshold static perimetric strategy with a large stimulus in the same automated perimeter used for FST may suffice. Use of broad-band chromatic filters in the perimeter provided an opportunity to determine the mediation of the light being perceived. If the goal of a clinical trial is to affect rod retinal pathways and the baseline pre-treatment results are all cone driven, a significant increase in sensitivity to the achromatic stimulus accompanied by a change in mediation from cone to rod could be an important observation. Phase I safety testing that would lead from baseline higher sensitivity with rod-mediated result to lower sensitivity with cone-mediated result should raise concerns about adverse effects. A caveat is that no change in achromatic sensitivity and mediation from baseline may be less readily interpreted. It may actually mean there was no change, or it could mean that there were regional increases or decreases in function that escaped detection because they occurred at sensitivities below the most sensitive retinal regions (which drive the FST response; Fig. 4).

Within- and inter-visit variability was studied for the FST. These results have no ready comparison in the literature. The closest comparison of techniques may be with the Goldmann–Weekers adaptometer (G–W), the time-honored and conventional clinical instrument that can be used to measure dark-adapted thresholds. G–W thresholds are usually determined with a 11° diameter target viewed centrally or eccentrically. Like most instruments using a diffusing bowl, including projection perimeters, the light source of the G–W cannot be completely confined to the target and there is some light scattering across the bowl. In a patient with unstable fixation and severe loss of visual sensitivity, the examination with the G–W may approximate that with the FST. Variability was reported as 6·75 dB ($n=29$) for dark-adapted thresholds measured with an 11° target located 7° below fixation (Birch et al., 1999), while there was an earlier report of 1·51 dB ($n=26$) for the same test but located centrally or in the superior field (Berson et al., 1985). The inter-visit variability results for FST of $\pm 3{\cdot}90$ dB fall between these published G–W estimates.

FST appears to be a suitable candidate perceptual outcome measure for clinical trials in subsets of patients that cannot perform dark-adapted perimetry. The technique should complement ERG and other measures, such as pupillometry (Aleman et al., 2004), and permits seriously impaired rod function to be quantified. Although the methods used in Experiments 1 and 2 are different and will serve different patient populations, it is of interest that the inter-visit variability of $\pm 3{\cdot}90$ dB from FST (representing the highest sensitivity in the retina under investigation) is not vastly different than $\pm 3{\cdot}04$ dB from the focal testing (representing the highest sensitivity loci in the profile). This suggests that such values may be the current best estimate of inter-visit variability for these types of psychophysical rod vision testing. Further advances in protocols and greater understanding of sources of variability may make dark-adapted threshold measurements an even less variable and more predictable monitor of rod function than previously considered.

Acknowledgements

This work was supported by the NIH/NEI, Macula Vision Research Foundation, Foundation Fighting Blindness, F.M. Kirby Foundation, Macular Disease Foundation, Research to Prevent Blindness and the Mackall Trust. We are grateful to Jessica Emmons, Alexander Sumaroka, Ilya Kniznik, Paul Schied, Mary Nguyen, Michael Pianta, Alexander Pantelyat, Andy Cheung, Boram Kim, Marisa Roman and Malgorzata Swider for critical help. Special thanks are due to Mr F. Letterio and members of Zeiss-Humphrey (Dublin, CA) who provided generous assistance and advice about how to modify the automated perimeter.

Appendix A. Modifications to an automated perimeter to perform the Full-field Stimulus Test (FST)

A commercially available automated perimeter (Humphrey Field Analyzer, model 750i, Zeiss-Humphrey, Dublin, CA) was modified to record psychophysical thresholds to full-field light stimuli under dark-adapted conditions (Fig. A1). A uniform full-field stimulus was produced by commanding the perimeter to project the light beam to a single inferior field locus ($x=0$, $y=-60°$) where a circular first surface mirror (25 mm diameter; Edmund Optics 32-945) was attached (Fig. A1(A) and (B)). The beam reflected by the mirror was pointed to a white diffuser at the top of the bowl which served to illuminate the bowl (Fig. A1(A) and (C)). The white diffuser (50×55 mm, cardboard painted matt white Sears #66108) was affixed to the yellow background illuminator window, covering it completely (Fig. A1(C)). A matt black cardboard baffle was installed below the chin rest (Fig. A1(A) and (B)) to block any spurious light from the mirror reaching the eye.

In order to perform dark-adapted testing, the background light of the instrument was turned off using a setup code provided from the manufacturer. This setup code works only under 'blue on yellow background' test condition which inserts the instrument's blue filter in the stimulus light path. To test with white light, the blue filter has to be moved out of the light path by lifting

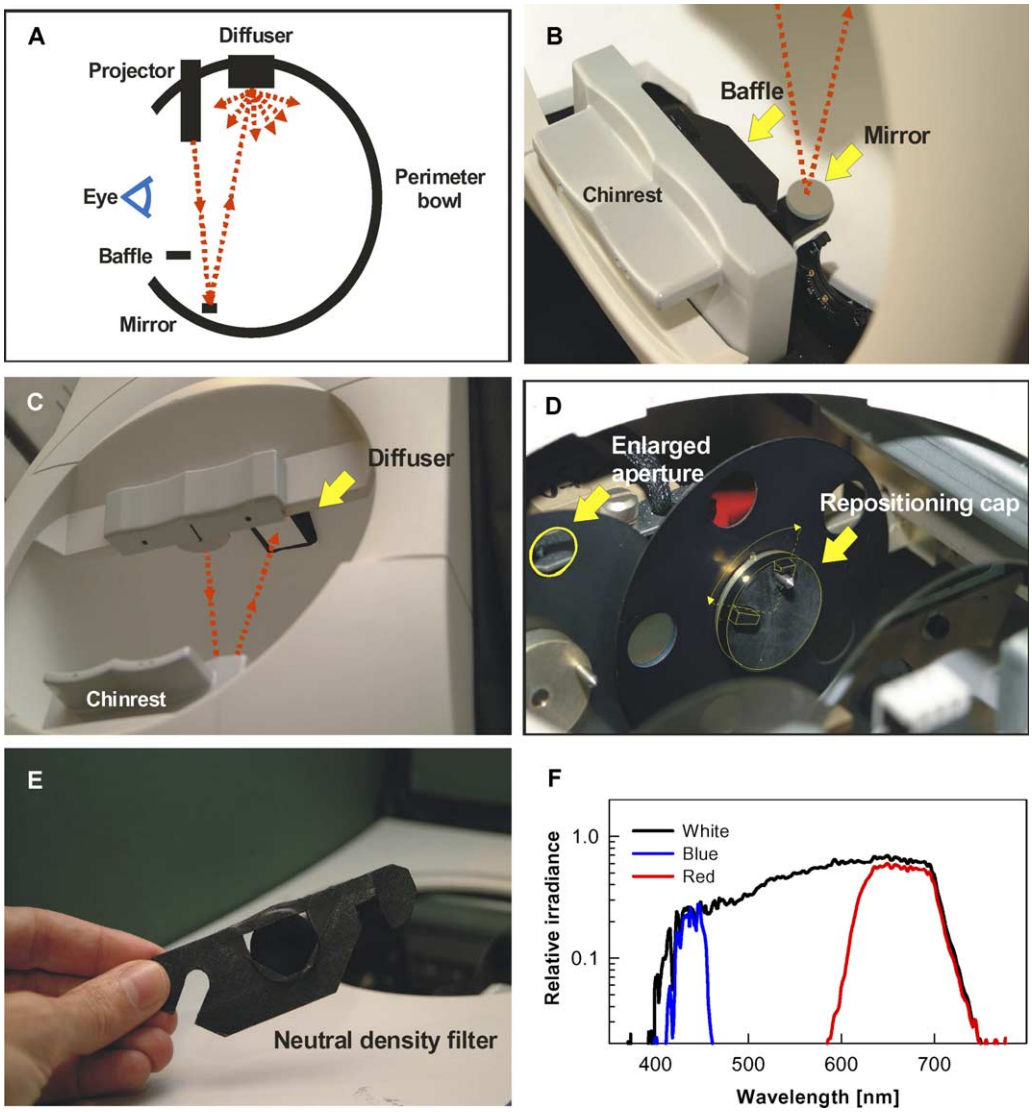

Fig. A1. Modifications to an automated perimeter to perform FST. (A) Schematic of perimeter bowl and light path from projector to mirror to diffuser. (B) Mirror and black baffle near and below chinrest (viewed from above). (C) Diffuser fixed to original yellow illuminator at top of bowl (viewed from below). (D) View with top cover of perimeter removed showing two adjacent wheels: aperture wheel with enlarged aperture is at left, and the colour filter wheel at right. A custom-made plastic repositioning cap is attached to the colour filter wheel to ensure that the instrument will test with white when programmed to test with blue. (E) A holder for a neutral density filter for the main light path. (F) Spectral characteristics of the broadband blue and red stimuli compared with the white light.

the hinged cover at the top of the instrument and rotating the filter wheel (Fig. A1(D)). The perimeter, however, automatically replaces the blue filter in the light path every time the operator cycles the machine to perform a new test. To avoid delays associated with manual rotation of the filter wheel, a custom-built plastic snap-on cap was designed to increase the preset rotation angle and make the instrument use an open filter slot instead of the blue filter. This repositioning cap can be fitted manually by pressure to the filter wheel body, thereby permitting repeated testing with white light and avoiding manual realignment of the filter wheel (Fig. A1(D)).

The dynamic range of the stimulus light was increased to be able to accommodate the extreme loss of visual sensitivity in patients with severe retinal degenerative diseases and still be able to test absolute rod sensitivity in normal subjects. The maximum luminance (0 dB stimulus level) was increased by enlarging the available aperture. The aperture wheel in the perimeter light path normally includes six openings: five Goldmann target sizes (I–V), and a wider opening, which is not used for conventional testing. An increase of available light level of about 6·5 dB can be obtained by using this larger opening instead of size V, but the software does not have an option to select this opening. Therefore, size II target was mechanically enlarged (Fig. A1(D)) recognizing that this modification eliminates future testing with this target. Using this enlarged aperture, mirror and diffuser, the maximum (0 dB) luminance was $3{\cdot}7\ \mathrm{cd\ m^{-2}}$, uniform to within 2 dB. To extend the low end of the stimulus dynamic range, a 3·0 log unit neutral density filter (Melles Griot #03 FNA 226, Carlsbad, CA) on a custom-built plastic filter holder was installed coaxial to the light beam (Fig. A1(E)). This filter was manually inserted prior to testing subjects with anticipated higher light sensitivity.

Stray light leaking from the projector enclosure was baffled by covering bowl openings with black masking tape (Jacobson et al., 1986). The lateral bowl opening used for the chin rest mechanism was shielded using a cardboard template and black felt. Rear ventilation openings were light-shielded with a hanging black curtain leaving ample room for air flow. The original yellow fixation LED was replaced by a red LED and attenuated until it was just visible to the subject, or turned off completely in subjects with no fixation (Jacobson et al., 1986). The infrared illuminators (for eye visualization) were disabled after head positioning, since part of the illumination fell within the visible range and may have disturbed dark adaptation in subjects with good sensitivities.

Custom test parameters used were as follows: strategy = full threshold; speed = slow; gaze tracking = off; fixation = central; stimulus size = II (corresponding to the enlarged aperture, see above); color = blue; background = yellow; single point at $x = 0$, $y = -60°$.

References

Acland, G.M., Aguirre, G.D., Ray, J., Zhang, Q., Aleman, T.S., Cideciyan, A.V., Pearce-Kelling, S.E., Anand, V., Zeng, Y., Maguire, A.M., Jacobson, S.G., Hauswirth, W.W., Bennett, J., 2001. Gene therapy restores vision in a canine model of childhood blindness. Nat. Genet. 28, 92–95.

Aleman, T.S., Jacobson, S.G., Chico, J.D., Scott, M.L., Cheung, A.Y., Windsor, E.A., Furushima, M., Redmond, T.M., Bennett, J., Palczewski, K., Cideciyan, A.V., 2004. Impairment of the transient pupillary light reflex in Rpe65(–/–) mice and humans with Leber congenital amaurosis. Invest. Ophthalmol. Vis. Sci. 45, 1259–1271.

Andreasson, S.O., Sandberg, M.A., Berson, E.L., 1988. Narrow-band filtering for monitoring low-amplitude cone electroretinograms in retinitis pigmentosa. Am. J. Ophthalmol. 105, 500–503.

Apathy, P.P., Jacobson, S.G., Nghiem-Phu, L., Knighton, R.W., Parel, J.-M., 1987. Computer-aided analysis in automated dark-adapted static perimetry, in: Greve, E.L., Heijl, A. (Eds.), Seventh International Visual Field Symposium. Martinus Nijhoff Publishers, Dordrecht, pp. 279–284.

Apfelstedt-Sylla, E., Kunisch, M., Horn, M., Ruther, K., Gal, A., Zrenner, E., 1992. Diffuse loss of rod function in autosomal dominant retinitis pigmentosa with pro-347-leu mutation of rhodopsin. Ger. J. Ophthalmol. 1, 319–327.

Berson, E.L., Sandberg, M.A., Rosner, B., Birch, D.G., Hanson, A.H., 1985. Natural course of retinitis pigmentosa over a three-year interval. Am. J. Ophthalmol. 99, 240–251.

Berson, E.L., Rosner, B., Sandberg, M.A., Hayes, K.C., Nicholson, B.W., Weigel-DiFranco, C., Willett, W., 1993. A randomized trial of vitamin A and vitamin E supplementation for retinitis pigmentosa. Arch. Ophthalmol. 111, 761–772.

Berson, E.L., Rosner, B., Weigel-DiFranco, C., Dryja, T.P., Sandberg, M.A., 2002. Disease progression in patients with dominant retinitis pigmentosa and rhodopsin mutations. Invest. Ophthalmol. Vis. Sci. 43, 3027–3036.

Berson, E.L., Rosner, B., Sandberg, M.A., Weigel-DiFranco, C., Moser, A., Brockhurst, R.J., Hayes, K.C., Johnson, C.A., Anderson, E.J., Gaudio, A.R., Willett, W.C., Schaefer, E.J., 2004. Clinical trial of docosahexaenoic acid in patients with retinitis pigmentosa receiving vitamin A treatment. Arch. Ophthalmol. 122, 1297–1305.

Bessant, D.A., Ali, R.R., Bhattacharya, S.S., 2001. Molecular genetics and prospects for therapy of the inherited retinal dystrophies. Curr. Opin. Genet. Dev. 11, 307–316.

Birch, D.G., Sandberg, M.A., 1997. Submicrovolt full-field cone electroretinograms: artifacts and reproducibility. Doc. Ophthalmol. 92, 269–280.

Birch, D.G., Herman, W.K., deFaller, J.M., Disbrow, D.T., Birch, E.E., 1987. The relationship between rod perimetric thresholds and full-field rod ERGs in retinitis pigmentosa. Invest. Ophthalmol. Vis. Sci. 28, 954–965.

Birch, D.G., Anderson, J.L., Fish, G.E., 1991. Longitudinal measures in children receiving ENCAD for hereditary retinal degeneration. Doc. Ophthalmol. 77, 185–192.

Birch, D.G., Anderson, J.L., Fish, G.E., 1999. Yearly rates of rod and cone functional loss in retinitis pigmentosa and cone-rod dystrophy. Ophthalmology 106, 258–268.

Birch, D.G., Hood, D.C., Locke, K.G., Hoffman, D.R., Tzekov, R.T., 2002. Quantitative electroretinogram measures of phototransduction in cone and rod photoreceptors: normal aging, progression with disease, and test–retest variability. Arch. Ophthalmol. 120, 1045–1051.

Bland, J.M., Altman, D.G., 1986. Statistical methods for assessing agreement between two methods of clinical measurement. Lancet 327, 307–310.

Bland, J.M., Altman, D.G., 1996. Measurement error. BMJ 313, 744.

Blumenthal, E.Z., Sample, P.A., Berry, C.C., Lee, A.C., Girkin, C.A., Zangwill, L., Caprioli, J., Weinreb, R.N., 2003. Evaluating several

sources of variability for standard and SWAP visual fields in glaucoma patients, suspects, and normals. Ophthalmology 110, 1895–1902.

Caruso, R.C., Nussenblatt, R.B., Csaky, K.G., Valle, D., Kaiser-Kupfer, M.I., 2001. Assessment of visual function in patients with gyrate atrophy who are considered candidates for gene replacement. Arch. Ophthalmol. 119, 667–669.

Chauhan, B.C., Johnson, C.A., 1999. Test-retest variability of frequency-doubling perimetry and conventional perimetry in glaucoma patients and normal subjects. Invest. Ophthalmol. Vis. Sci. 40, 648–656.

Cideciyan, A.V., Hood, D.C., Huang, Y., Banin, E., Li, Z.Y., Stone, E.M., Milam, A.H., Jacobson, S.G., 1998. Disease sequence from mutant rhodopsin allele to rod and cone photoreceptor degeneration in man. Proc. Natl Acad. Sci. USA 95, 7103–7108.

Cideciyan, A.V., Aleman, T.S., Swider, M., Schwartz, S.B., Steinberg, J.D., Brucker, A.J., Maguire, A.M., Bennett, J., Stone, E.M., Jacobson, S.G., 2004. Mutations in ABCA4 result in accumulation of lipofuscin before slowing of the retinoid cycle: a reappraisal of the human disease sequence. Hum. Mol. Genet. 13, 525–534.

Cornsweet, T.N., 1970. Visual Perception. Academic Press, New York pp. 6–26.

Curcio, C.A., Medeiros, N.E., Millican, C.L., 1996. Photoreceptor loss in age-related macular degeneration. Invest. Ophthalmol. Vis. Sci. 37, 1236–1249.

Dagnelie, G., Massof, R.W., 1994. Sub-microvolt electroretinograms: negotiating the pitfalls of photoelectricity and noise, in: Vision Science and Its Applications, 1994 Technical Digest Series, vol. 2. Optical Society of America, Washington, DC pp. 354–357.

de Juan Jr., E., Cooney, M.J., Humayun, M.S., Jensen, P.S., 1999. Treatment of retinal disease in the new millennium. Ophthalmol. Clin. North Am. 23, 539–562.

Delyfer, M.N., Leveillard, T., Mohand-Said, S., Hicks, D., Picaud, S., Sahel, J.A., 2004. Inherited retinal degenerations: therapeutic prospects. Biol. Cell 96, 261–269.

Ernst, W., Faulkner, D.J., Hogg, C.R., Powell, D.J., Arden, G.B., Vaegan, 1983. An automated static perimeter/adaptometer using light emitting diodes. Br. J. Ophthalmol. 67, 431–442.

Flynn, M.F., Fishman, G.A., Anderson, R.J., Roberts, D.K., 2001. Retrospective longitudinal study of visual acuity change in patients with retinitis pigmentosa. Retina 21, 639–646.

Glovinsky, Y., Quigley, H.A., Drum, B., Bissett, R.A., Jampel, H.D., 1992. A whole-field scotopic retinal sensitivity test for the detection of early glaucoma damage. Arch. Ophthalmol. 110, 486–490.

Gordon, M.O., Kass, M.A., 1999. The ocular hypertension treatment study: design and baseline description of the participants. Arch. Ophthalmol. 117, 573–583.

Grover, S., Fishman, G.A., Birch, D.G., Locke, K.G., Rosner, B., 2003. Variability of full-field electroretinogram responses in subjects without diffuse photoreceptor cell disease. Ophthalmology 110, 1159–1163.

Gunkel, R.D., 1967. Retinal profiles, A psychophysical test of rod and cone sensitivity. Arch. Ophthalmol. 77, 22–25.

Hirakawa, H., Iijima, H., Gohdo, T., Imai, M., Tsukahara, S., 1999. Progression of defects in the central 10-degree visual field of patients with retinitis pigmentosa and choroideremia. Am. J. Ophthalmol. 127, 436–442.

Hoffman, D.R., Locke, K.G., Wheaton, D.H., Fish, G.E., Spencer, R., Birch, D.G., 2004. A randomized, placebo-controlled clinical trial of docosahexaenoic acid supplementation for X-linked retinitis pigmentosa. Am. J. Ophthalmol. 137, 704–718.

Holopigian, K., Greenstein, V., Seiple, W., Carr, R.E., 1996. Rates of change differ among measures of visual function in patients with retinitis pigmentosa. Ophthalmology 103, 398–405.

Humayun, M.S., de Juan Jr., E., del Cerro, M., Dagnelie, G., Radner, W., Sadda, S.R., del Cerro, C., 2000. Human neural retinal transplantation. Invest. Ophthalmol. Vis. Sci. 41, 3100–3106.

Humayun, M.S., Weiland, J.D., Fujii, G.Y., Greenberg, R., Williamson, R., Little, J., Mech, B., Cimmarusti, V., Van Boemel, G., Dagnelie, G., de Juan, E., 2003. Visual perception in a blind subject with a chronic microelectronic retinal prosthesis. Vis. Res. 43, 2573–2581.

Jacobson, S.G., Voigt, W.J., Parel, J.M., Apathy, P.P., Nghiem-Phu, L., Myers, S.W., Patella, V.M., 1986. Automated light- and dark-adapted perimetry for evaluating retinitis pigmentosa. Ophthalmology 93, 1604–1611.

Jacobson, S.G., Yagasaki, K., Feuer, W.J., Roman, A.J., 1989. Interocular asymmetry of visual function in heterozygotes of X-linked retinitis pigmentosa. Exp. Eye Res. 48, 679–691.

Jacobson, S.G., Kemp, C.M., Sung, C.H., Nathans, J., 1991. Retinal function and rhodopsin levels in autosomal dominant retinitis pigmentosa with rhodopsin mutations. Am. J. Ophthalmol. 112, 256–271.

Jacobson, S.G., Cideciyan, A.V., Iannaccone, A., Weleber, R.G., Fishman, G.A., Maguire, A.M., Affatigato, L.M., Bennett, J., Pierce, E.A., Danciger, M., Farber, D.B., Stone, E.M., 2000. Disease expression of RP1 mutations causing autosomal dominant retinitis pigmentosa. Invest. Ophthalmol. Vis. Sci. 41, 1898–1908.

Jacobson, S.G., Sumaroka, A., Aleman, T.S., Cideciyan, A.V., Schwartz, S.B., Roman, A.J., McInnes, R.R., Sheffield, V.C., Stone, E.M., Swaroop, A., Wright, A.F., 2004. Nuclear receptor NR2E3 gene mutations distort human retinal laminar architecture and cause an unusual degeneration. Hum. Mol. Genet. 13, 1893–1902.

Katz, J., Sommer, A., 1988. Reliability indexes of automated perimetric tests. Arch. Ophthalmol. 106, 1252–1254.

Katz, J., Sommer, A., 1990. Reliability of automated perimetric tests. Arch. Ophthalmol. 108, 777–778.

Keltner, J.L., Johnson, C.A., Spurr, J.O., Beck, R.W., 1999. Comparison of central and peripheral visual field properties in the optic neuritis treatment trial. Am. J. Ophthalmol. 128, 543–553.

LaVail, M.M., Yasumura, D., Matthes, M.T., Lau-Villacorta, C., Unoki, K., Sung, C.H., Steinberg, R.H., 1998. Protection of mouse photoreceptors by survival factors in retinal degenerations. Invest. Ophthalmol. Vis. Sci. 39, 592–602.

Lodha, N., Westall, C.A., Brent, M., Abdolell, M., Heon, E., 2003. A modified protocol for the assessment of visual function in patients with retinitis pigmentosa. Adv. Exp. Med. Biol. 533, 49–57.

Lyness, A.L., Ernst, W., Quinlan, M.P., Clover, G.M., Arden, G.B., Carter, R.M., Bird, A.C., Parker, J.A., 1985. A clinical, psychophysical, and electroretinographic survey of patients with autosomal dominant retinitis pigmentosa. Br. J. Ophthalmol. 69, 326–339.

Marc, R.E., Jones, B.W., Watt, C.B., Strettoi, E., 2003. Neural remodeling in retinal degeneration. Prog. Retin. Eye Res. 22, 607–655.

Margalit, E., Maia, M., Weiland, J.D., Greenberg, R.J., Fujii, G.Y., Torres, G., Piyathaisere, D.V., O'Hearn, T.M., Liu, W., Lazzi, G., Dagnelie, G., Scribner, D.A., de Juan Jr., E., Humayun, M.S., 2002. Retinal prosthesis for the blind. Surv. Ophthalmol. 47, 335–356.

Marmor, M.F., Aguirre, G., Arden, G., Berson, E., Birch, D.G., Boughman, J.A., Carr, R., Chatrian, G.E., del Monte, M., Dowling, J., Enoch, J., Fishman, G.A., Fulton, A.B., Garcia, C.A., Gouras, P., Heckenlively, J., Hu, D., Lewis, R.A., Niemeyer, G., Parker, J.A., Perlman, I., Ripps, H., Sandberg, M.A., Siegel, I., Weleber, R.G., Wolf, M.L., Wu, L., Young, R.S.L., 1983. Retinitis pigmentosa: a symposium on terminology and methods of examination. Ophthalmology 90, 126–131.

Massof, R.W., Finkelstein, D., 1979. Rod sensitivity relative to cone sensitivity in retinitis pigmentosa. Invest. Ophthalmol. Vis. Sci. 18, 263–272.

Owsley, C., Jackson, G.R., Cideciyan, A.V., Huang, Y., Fine, S.L., Ho, A.C., Maguire, M.G., Lolley, V., Jacobson, S.G., 2000. Psychophysical evidence for rod vulnerability in age-related macular degeneration. Invest. Ophthalmol. Vis. Sci. 41, 267–273.

Peters, A.Y., Locke, K.G., Birch, D.G., 2000. Comparison of the Goldmann-Weekers dark adaptometer and LKC technologies scotopic sensitivity tester-1. Doc. Ophthalmol. 101, 1–9.

Reus, N.J., Lemij, H.G., 2004. The relationship between standard automated perimetry and GDx VCC measurements. Invest. Ophthalmol. Vis. Sci. 45, 840–845.

Sieving, P.A., Arnold, E.B., Jamison, J., Liepa, A., Coats, C., 1998. Submicrovolt flicker electroretinogram: cycle-by-cycle recording of multiple harmonics with statistical estimation of measurement uncertainty. Invest. Ophthalmol. Vis. Sci. 39, 1462–1469.

Spry, P.G., Johnson, C.A., 2002. Identification of progressive glaucomatous visual field loss. Surv. Ophthalmol. 47, 158–173.

Spry, P.G., Johnson, C.A., McKendrick, A.M., Turpin, A., 2001. Variability components of standard automated perimetry and frequency-doubling technology perimetry. Invest. Ophthalmol. Vis. Sci. 42, 1404–1410.

Weleber, R.G., Kurz, D.E., Trzupek, K.M., 2003. Treatment of retinal and choroidal degenerations and dystrophies: current status and prospects for gene-based therapy. Ophthalmol. Clin. North Am. 16, 583–593.

Wong, F., 1997. Investigating retinitis pigmentosa: a laboratory scientist's perspective. Prog. Retin. Eye Res. 16, 353–373.